Introducing Selenium in Single-Component Molecular Conductors Based on Nickel Bis(dithiolene) Complexes

Hadi Hachem, Hengbo Cui, Reizo Kato, Olivier Jeannin, F Barriere, Marc Fourmigué, Dominique Lorcy

Introducing selenium in single-component molecular conductors based on nickel bis(dithiolene) complexes

Hadi Hachem, HengBo Cui, Reizo Kato,* Olivier Jeannin, Frédéric Barrière, Marc Fourmigué,* and Dominique Lorcy*

ABSTRACT. Two selenated analogs of the all-sulfur [Ni(Et-thiazdt)$_2$] single-component molecular conductor (Et-thiazdt: N-ethyl-thiazoline-2-thione-4,5-dithiolate) have been prepared from their precursor radical anion complexes. Replacement of the thione by a selenone moiety gives the neutral [Ni(Et-thiaz**Se**dt)$_2$] complex. It adopts an unprecedented solid-state organization (for neutral nickel complexes), with the formation of perfectly eclipsed dimers and very short intermolecular Se•••Se contacts (81% of the van der Waals contact distance). Limited interactions between dimers leads to a large semiconducting gap and low conductivity (σ_{RT} = 1.7×10^{-5} S.cm^{-1}). On the other hand, going from the neutral [Ni(Et-thiazdt)$_2$] dithiolene to the corresponding [Ni(Et-thiaz**ds**)$_2$] diselenolene complex gives rise to a more conventional layered structure built out of uniform stacks of the diselenolene complexes, different however from the all-sulfur analog [Ni(Et-thiazdt)$_2$]. Band structure calculations show an essentially 1D electronic structure with large band dispersion and small HOMO-LUMO gap. Under high pressures (up to 19 GPa), the conductivity increases by four orders of magnitude and the activation energy is decreased from 120 meV to only 13 meV, with an abrupt change observed around 10 GPa, suggesting a structural phase transition under pressure.

INTRODUCTION

Following years of extensive studies dedicated to conducting molecular materials derived from charge-transfer salts and ion-radical salts, more recent advances relate to the so-called single-component molecular conductors, i.e. highly conducting crystalline systems based on one single molecular entity. Essentially two approaches were followed in this young domain, molecular radical (S = ½) species (be they organic molecules[1,2,3] or coordination complexes), or formally closed-shell, neutral dithiolene complexes derived from the extended tetrathiafulvalenedithiolate ligand and analogs.[4,5,6] The radical approach (Chart 1a) assumes that upon packing, a half-filled conduction band forms,[7,8] allowing for metallic conductivity as in the zwitterionic TTF-extended dicarboxylate radical (TED).[9] This approach is often thwarted by the strong propensity of such radical systems to dimerize (as in the Peierls or the Spin-Peierls transitions), leading to a semiconducting gap and low conductivity. Recent examples of organic compounds include quinone-bridged bis(dithiazolyl) radicals,[10] hydrogen-bonded bis(TTF-catechol).[11] Among coordination complexes (Chart 1b), radical bis(dithiolene) gold complexes[12] can adopt non-dimerized structures[13,14] and become metallic, upon application of pressure,[15,16] or even at ambient pressure in $[Au(Me\text{-}thiazdt)_2]^{\bullet}$.[17] The second main approach to single-component molecular conductors is based on formally closed-shell complexes such as $[Ni(tmdt)_2]$ and analogs (Chart 1b)[4,5,6] where the highly delocalized tmdt ligand allows for extensive intermolecular interactions and truly 3D band structures. In that respect, smaller neutral closed-shell nickel dithiolene complexes such as the prototypical $[Ni(dmit)_2]^0$ (Chart 1b) were known to behave as "normal" semiconductors[18,19] until some of us recently demonstrated that application of high pressures could turn them into a metallic state,[20] due to increased band dispersions, up to the point where the Fermi level can cross both HOMO and LUMO bands (but at different k_F values to hinder avoided band crossing effects and gap opening).

Chart 1. Molecular structures of single-component conductors

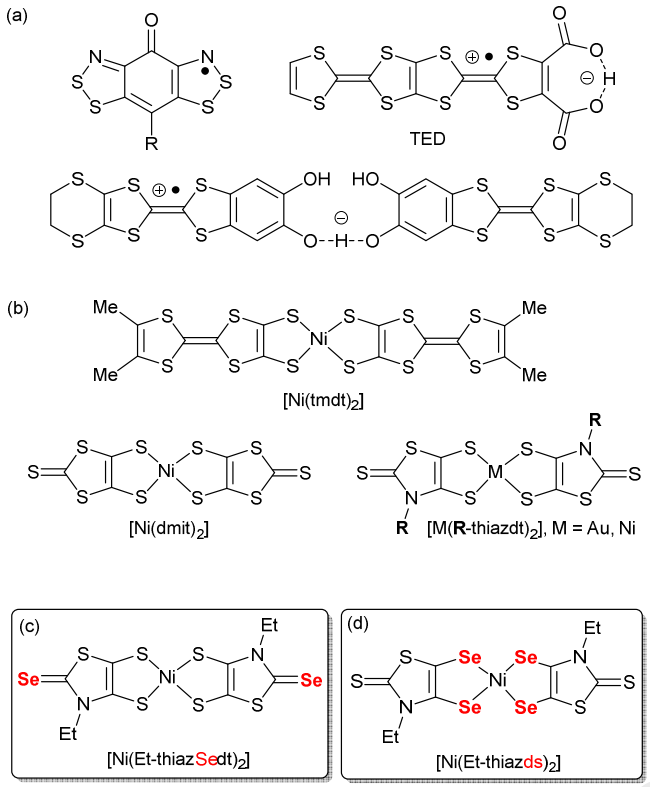

Based on this preliminary attractive result, we recently considered nickel dithiolene complexes derived from the thiazolinedithiolate ligand R-thiazdt. Indeed, such complexes with gold, that is $[Au(R\text{-thiazdt})_2]^{\bullet}$ (Chart 1b) proved to be excellent single-component molecular conductors (following the first approach detailed above).[15–17] Accordingly, the ethyl-substituted complex nickel complex, $[Ni(Et\text{-thiazdt})_2]^0$ was found to organize into uniform chains and, albeit a semi-conductor at ambient pressure ($\sigma_{RT} = 4.3 \times 10^{-4}$ S/cm), to become metallic at low temperature at 4.4 GPa and metallic over the whole temperature range over 6.9 GPa.[21] In order to explore further this family and its behavior under pressure, we considered the possibility to substitute sulfur atoms for selenium ones, as such substitutions are well known to increase the band dispersion in molecular conducting systems.[16] In that respect, sulfur atoms can be easily replaced by selenium ones in the R-thiazdt skeleton, either by replacing the outer thione moiety by a selenone to give the R-thiaz**Se**dt dithiolene ligand (Chart 1c), or by replacing the two coordinating sulfur atoms by selenium ones to give the corresponding R-thiaz**ds** diselenolene ligand (Chart 1d). We have successfully explored these two modifications on the N-ethyl substituted nickel complex $[Ni(Et\text{-thiazdt})_2]^0$, to give respectively the two neutral complexes $[Ni(Et\text{-thiaz}\mathbf{Se}dt)_2]^0$, and $[Ni(Et\text{-thiaz}\mathbf{ds})_2]^0$. In the following, we will describe the syntheses and properties of the monoanionic precursor complexes, their electrocrystallization to the

neutral complexes with their structural and electronic properties, in comparison to those of the reference, all sulfur [Ni(Et-thiazdt)$_2$] single-component molecular conductor.

■ RESULTS AND DISCUSSION

The strategy used to form the anionic complexes is similar to that used to synthesize the analogous gold complexes (Scheme 1). The protected dithiolene form of the selenone **3** was prepared from the N-ethyl-thiazoline-2-thione **1**, according to a modified procedure described earlier for the N-isopropyl analogue.[22] Reaction of **1** with MeI and NaHSe provides the N-Et-1,3-thiazoline-2-selenone **2**, which is easily converted into the protected dithiolene **3** after the subsequent addition of LDA, sulfur and bromopropionitrile. Deprotection with NaOMe generates the air-sensitive dithiolate which reacts with $NiCl_2$•$6H_2O$ and NBu_4Br to afford, after air oxidation, the monoanionic dithiolene complex [Ni(Et-thiaz**Se**dt)$_2$]$^{-1}$, isolated as the Bu_4N^+ salt in 31% yield. A similar reaction involving the known protected diselenolene **4**[16] affords the monoanionic diselenolene complex [Ni(Et-thiaz**ds**)$_2$]$^{-1}$, isolated as the Ph_4P^+ salt in 52% yield.

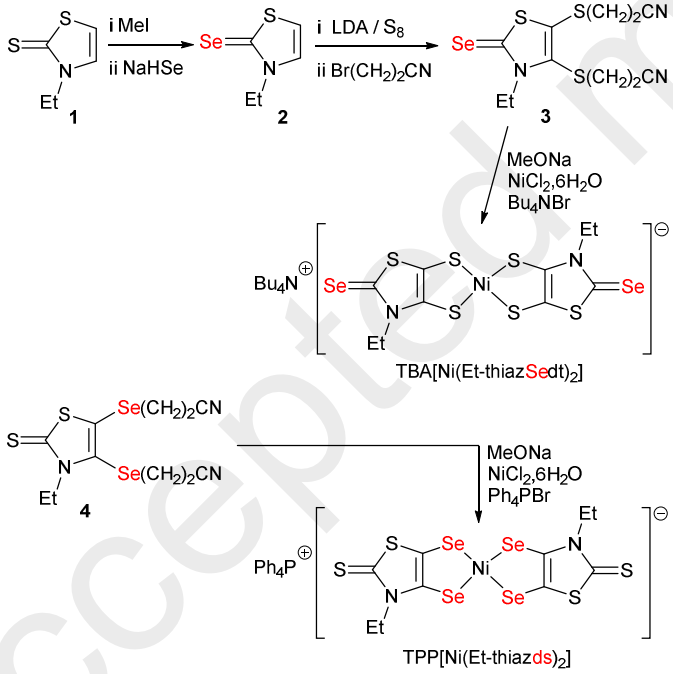

Scheme 1. Syntheses of the anionic complexes [Ni(Et-thiazSedt)$_2$]$^-$ and [Ni(Et-thiazds)$_2$]$^-$.

Electrochemical properties were investigated by cyclic voltammetry in CH_2Cl_2 (Table 1). The two novel anionic complexes exhibit two chemically reversible electron transfers associated with the −2/−1 and −1/0 redox states, while the 0/+1 electron transfer is quasi-reversible. Comparison with the all-sulfur dithiolene analog [Ni(Et-thiazdt)$_2$] shows a recurrent anodic

shift induced by the introduction of selenium, with a stronger effect on the diselenolene complex. This behavior has been already rationalized on the basis of theoretical studies (DFT) on dmit complexes and their Se-analogs.[23] Besides, we note that the 0/+1 quasi-reversible oxidation process is found at lower potential for the [Ni(Et-thiaz**Se**dt)$_2$] complex.

Table 1 Redox properties of the complexes in CH_2Cl_2 with [NBu_4][PF_6] 0.1 M, E in V *vs*. SCE with scan rate = 100 mV.s^{-1}. ΔE stands for [$E_{1/2}$ (−1/0) − $E_{1/2}$(−2/−1)].

Complex	$E_{1/2}$(−2/−1)	$E_{1/2}$ (−1/0)	ΔE	E_{pa}/E_{pc}(0/+1)
[PPh_4][Ni(Et-thiazdt)$_2$]	−0.33	+0.20	0.53	+1.08/+0.99
[NBu_4][Ni(Et-thiaz**Se**dt)$_2$]	−0.28	+0.24	0.52	+0.76/+0.63
[PPh_4][Ni(Et-thiaz**ds**)$_2$]	−0.30	+0.27	0.57	+1.03/+0.84

Depending on their oxidation state, nickel bis(dithiolene) (and diselenolene) complexes are known to present extremely intense near-infrared (NIR) electronic transitions,[24] of potential interest for the elaboration of optoelectronic devices.[25, 26] UV-vis-NIR spectroscopic investigations, carried out on the monoanionic complexes allowed us to determine the absorption maxima (λ_{max}) and extinction coefficient (ε) of these NIR absorption bands. On the other hand, the insolubility of the neutral species hinders such measurements and absorption maxima were determined from spectroelectrochemical investigations (Figure 1). As anticipated, the radical anion species exhibit low energy absorption bands in the range 1200-1300 nm, shifted to higher energy in the neutral complexes (1000-1100 nm). There again, comparison of the UV-vis NIR spectra shows some discrepancies between the all-sulfur dithiolene neutral complex [Ni(Et-thiazdt)$_2$] and the one with selenium atoms, especially in the optical band gap. The presence of the selenium atoms induces a shift towards lower energies for the λ_{onset} and thus a decrease of the optical band gap (Eg from 1.03 eV for [Ni(Et-thiazdt)$_2$] to 0.88 eV for [Ni(Et-thiazds)$_2$].

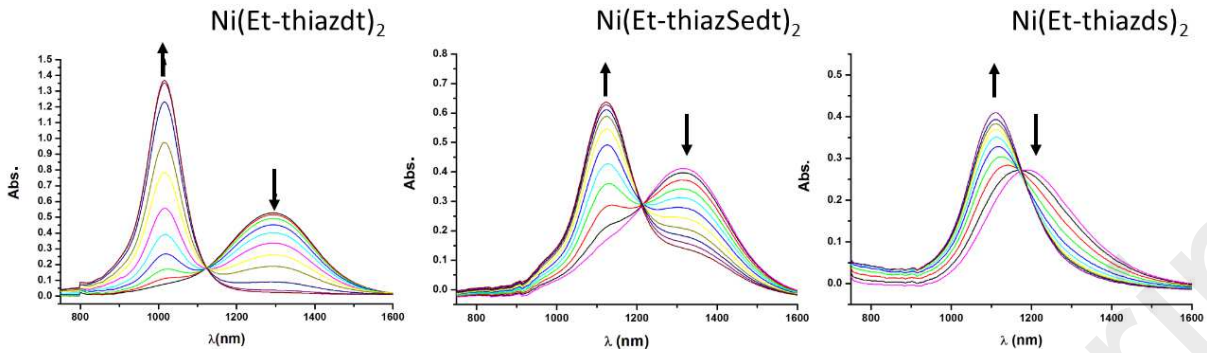

Figure 1. UV-vis-NIR absorption spectra monitored electrochemically from the monoanionic state to the neutral state of $[Ni(Et\text{-}thiazdt)_2]^{-1}$ (left), $[Ni(Et\text{-}thiaz\mathbf{Se}dt)_2]^{-1}$ (middle) and $[Ni(Et\text{-}thiaz\mathbf{ds})_2]^{-1}$ (right) in CH_2Cl_2, with 0.2 M NBu_4PF_6 as a supporting electrolyte.

Table 2. Wavelength of the absorption maxima and the corresponding molar extinction coefficients of the described complexes in their monoanionic radical and neutral states in the near infrared region

	λ_{max} (nm) (ε, $M^{-1}.cm^{-1}$)	λ_{max} (nm)
	monoanion	neutral complex
$[Ni(Et\text{-}thiazdt)_2]^{-1,0}$	1280 (21 000) [(a)]	1022
$[Ni(Et\text{-}thiaz\mathbf{Se}dt)_2]^{-1,0}$	1308 (26 900) [(b)]	1120
$[Ni(Et\text{-}thiaz\mathbf{ds})_2]^{-1,0}$	1186 (18 927) [(a)]	1082

[(a)]as Ph_4P^+ salt. [(b)]as Bu_4N^+ salt

The neutral complexes were obtained by electrocrystallization of the monoanionic salts in the presence of Et_4NPF_6 (0.2 M) in different solvents. Good quality crystals of [Ni(Et-thiaz**Se**dt)] were isolated in 1,1,2-tricholoroethane while $[Ni(Et\text{-}thiaz\mathbf{ds})_2]$ was best electrocrystallized from a CH_3CN/CH_2Cl_2 (7/2) mixture. In the following, we will first describe the crystal structures and magnetic properties of the monoanionic salts, and then the structural and electronic properties of the novel single-component molecular conductors isolated from their $1e^-$ oxidation.

$[NBu_4][Ni(Et\text{-}thiaz\mathbf{Se}dt)_2]$ crystallizes in the triclinic system, space group $P\bar{1}$, with both anion and cation in general position. As shown in Figure 2, the anionic dithiolene complex adopts a *cis* configuration, with a small distortion from planarity as the angle between both metallacycles amounts to 7.5(1)°. This *cis* configuration is quite rare in nickel bis(dithiolene) complexes but is essentially a result of the solid state organization. Indeed, gas phase geometry

optimizations with DFT [B3LYP/LanL2DZ] of the complex in the neutral or monoanion states show that both configurations are isoenergetic. In the solid state, Bu_4N^+ cations and radical anions are segregated into layers perpendicular to the *a* axis (Figure S1). Within the layers, only one intermolecular S•••S contact shorter than the sum of the van der Waals radii (3.49 Å) is found involving the sulfur atoms of the outer thiazoline ring. The temperature dependence of the magnetic susceptibility of the compound is well fitted to Curie-Weiss behavior (Figure S2), with a Curie constant of 0.356, and a θ value of –0.1 K, demonstrating the absence of sizeable magnetic interactions between the $S = ½$ radical anion species.

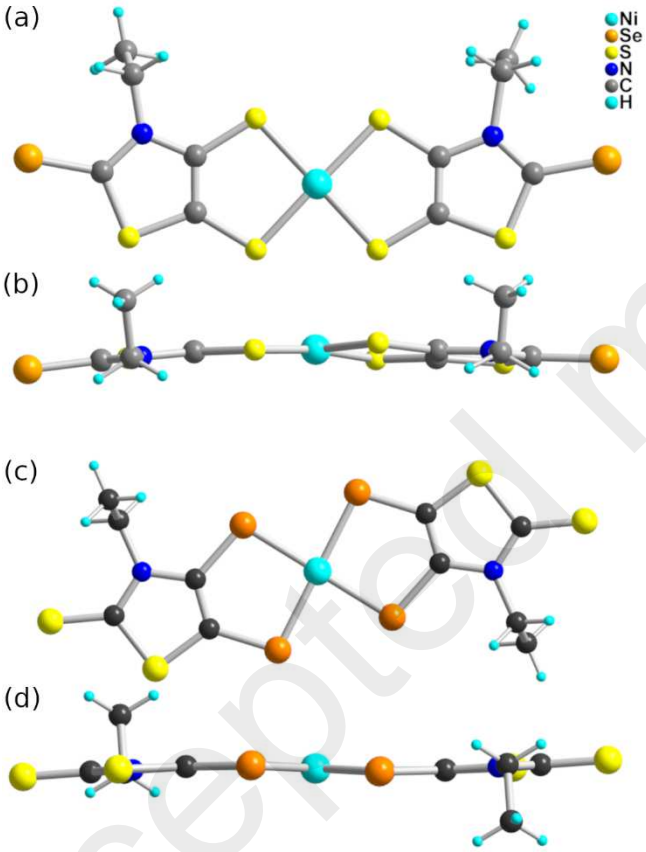

Figure 2. Details of the molecular structures of the anionic [Ni(Et-thiaz**Se**dt)$_2$] (a,b) and [Ni(Et-thiaz**ds**)$_2$]$^{-1}$ (c,d) complexes.

[Ph_4P][Ni(Et-thiaz**ds**)$_2$] crystallizes in the triclinic system, space group $P\bar{1}$, with two crystallographically independent anionic complexes, each of them on inversion centers, and one Ph_4P^+ cation in general position. Both crystallographically independent complexes adopt a *trans* configuration. In the solid state they are essentially separated from each other by the bulky Ph_4P^+ cations (Figure S3), thus impeding any sizeable intermolecular interactions between the

S = ½ radical species. The shortest intermolecular chalcogen-chalcogen contacts exceed 3.90 Å. It is also confirmed by the temperature dependence of the magnetic susceptibility, properly fitted by a Curie-Weiss behavior with θ = –1.5 K (Figure S4). The Curie constant was found at 0.410, giving a g value of 2.092. This value is in line with what is usually found in such nickel diselenolene complexes (2.088-2.093).[27]

Table 3. Bond distances within the metallacycles in both anionic and neutral complexes. θ is the folding angle of the metallacycle among the S---S (Se---Se) hinge within each metallacycle.

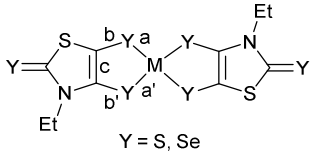

	a	a'	b	b'	c	θ	Ref
$[Ni(Et\text{-}thiazdt)_2]^{-1}$	2.1778(6)	2.11560(6)	1.722(2)	1.712(2)	1.356(3)	2.0	21a
$[Ni(Et\text{-}thiazdt)_2]^{0}$	2.1580(6)	2.1577(6)	1.685(2)	1.700(2)	1.388(3)	0.23	21a
$[Ni(Et\text{-}thiazdt)_2]^{0}$	2.1570(9)	2.1561(9)	1.679(3)	1.697(3)	1.389(4)	0.24	21b
$[Ni(Et\text{-}thiaz\mathbf{ds})_2]^{-1}$ (a)	2.2873(4)	2.2657(4)	1.863(4)	1.870(4)	1.337(5)	2.09	this work
	2.2936(5)	2.2816(5)	1.869(5)	1.873(4)	1.338(6)	3.75	
$[Ni(Et\text{-}thiaz\mathbf{ds})_2]^{0}$	2.2599(14)	2.2807(13)	1.813(12)	1.845(11)	1.386(16)	1.27	this work
$[Ni(Et\text{-}thiaz\mathbf{Sed}t)_2]^{-1}$ (b)	2.1545(13)	2.1599(16)	1.696(5)	1.704(5)	1.367(7)	1.53	this work
	2.1518(14)	2.1606(14)	1.713(5)	1.717(5)	1.352(7)	1.74	
$[Ni(Et\text{-}thiaz\mathbf{Se}dt)_2]_2^{0}$	2.1935(15)	2.1826(16)	1.691(5)	1.699(5)	1.403(7)	2.67	this work
	2.1813(15)	2.1933(16)	1.682(5)	1.691(5)	1.408(8)	3.30	

(a) Two independent metallacycles. (b) Two complexes, each on inversion center

The neutral complexes obtained from electrocrystallization experiments both crystallize in the triclinic system, space group $P\bar{1}$ but are not isostructural. They also differ from the two crystal structures reported for the all-sulfur analog, i.e. $[Ni(Et\text{-}thiazdt)_2]$.[21]

In $[Ni(Et\text{-}thiaz\mathbf{Se}dt)_2]$, the complex in general position in the unit cell adopts the *trans* configuration. Intramolecular bond distances (Table 3) confirm the oxidized character of the neutral complex, with the shortening of the Ni−S and C=C bonds and concomitant lengthening of the C−S bonds, when compared with those within the radical anion species $[Ni(thiaz\mathbf{Se}dt)_2]^{-1}$ (Cf Table 3). The complexes form dimers related by an inversion center in a perfectly eclipsed

overlap (Figure 3), with a short Ni•••Ni distance at 3.299(6) Å and an extremely short intra-dimer Se•••Se contact, 3.10 Å, that is 81% of the Se•••Se van der Waals contact distance (3.80 Å). Such a strong dimerization is quite surprising here with a formally closed-shell neutral nickel complex, while it is usually more frequently encountered in open-shell mixed-valence Ni/Pd/Pt complexes or in radical gold complexes. We believe that the outer selenium atoms play here a crucial role in stabilizing such eclipsed dimers. On the other hand, there are no example of such short Se•••Se contacts in the few reported structures of analogous complexes with an outer selenone moiety, as with the dmise (2-selenoxo-1,3-dithiole-4,5-dithiolate)[28] or the all-selenium $C_3Se_5^{2-}$ ligands.[29] This apparent unusual crystal arrangement as stacked dimers has been investigated by DFT calculations (B3LYP/LanLD2Z, Gaussian 09, version D01, supporting information). The optimized dimer is found to be stabilized by 0.18 eV compared to the energy of two isolated monomers. This stabilization is more significant than for the optimized geometry of a stacked dimer analogue with sulfur in place of selenium (only 0.03 eV). This stabilization, together with the electronic structure of the dimer *vs* the monomer (supporting information), indicates that such a structural organization may not be that uncommon among many possible stabilizing interactions in a crystal, especially for molecules displaying Se•••Se interactions.

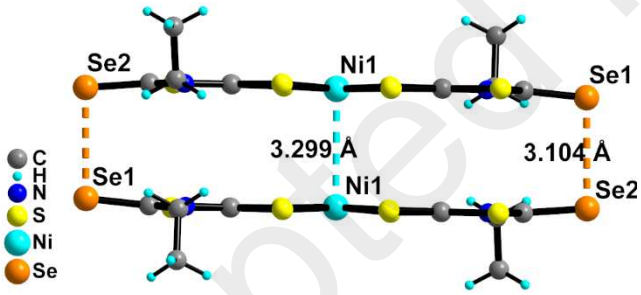

Figure 3. Detail of one dimer in the structure of [Ni(Et-thiaz**Se**dt)$_2$].

In the crystal, the dimers stack along the *b*-axis and interact sideway along *a*-axis, forming layers in the *ab* plane, that alternate along *c* axis (Figure 4a), with inter-layer Se•••Se contacts at 3.753(6) at 3.628(5), below the Se•••Se van der Waals contact distance at 3.80 Å (Figure 4b).

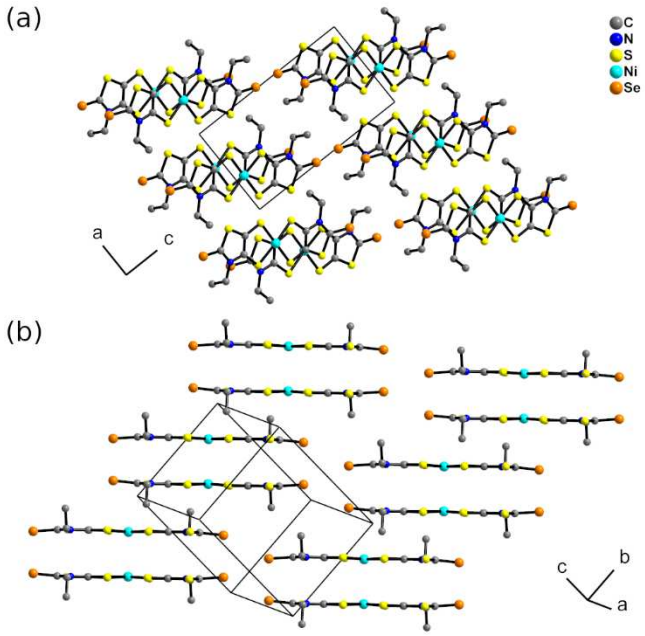

Figure 4 Solid state structure of neutral [Ni(Et-thiaz**Se**dt)$_2$], (a) viewed along the *b* stacking axis and (b) showing the stacks running along *b*.

Six different intermolecular interactions are identified (Figure 5). Interactions I and II run along the stacks, interactions III and IV between the stacks along *a*, and interactions V and VI between the layers through these Se•••Se contacts. The energies of the overlap interactions between the frontier orbitals are collected in Table 4. These β_{ij} interaction energies[30] have been extensively used by Whangbo[31] and Canadell[32] to discuss the electronic structure of molecular conductors. The strongest interaction is the intra-dimer HOMO-HOMO and LUMO-LUMO overlaps (Interaction I) while interaction II gives a 1D character to this compound.

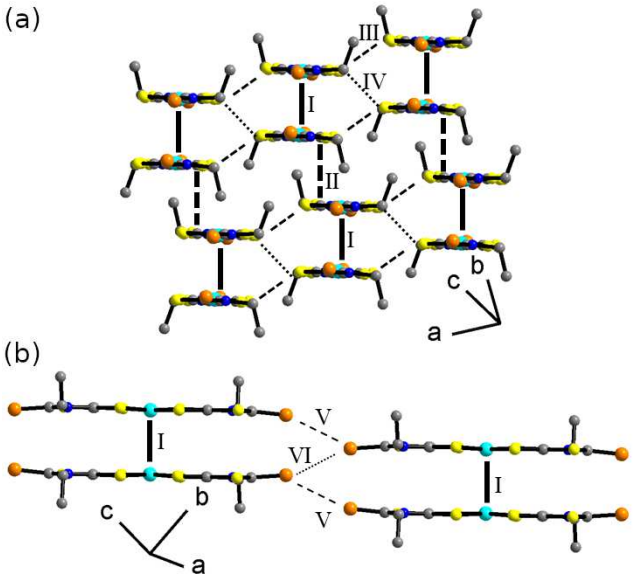

Figure 5 Inter and intra-stack interactions in [Ni(Et-thiaz**Se**dt)$_2$]$_2$

Table 4 Intermolecular interaction energies in [Ni(Et-thiaz**Se**dt)$_2$]$_2$ (in eV). See Figure 5 for interacting molecules.

	HOMO-HOMO	HOMO-LUMO	LUMO-HOMO	LUMO-LUMO
Int **I**	−1.3244	−0.0357	−0.0357	+1.0351
Int **II**	−0.2124	−0.1266	−0.1266	−0.0520
Int **III**	+0.0044	+0.0021	+0.0049	−0.0049
Int **IV**	−0.0246	+0.0027	+0.0027	−0.0142
Int **V**	+0.0045	+0.0039	−0.0026	−0.0024
Int **VI**	+0.0220	−0.0146	−0.0146	+0.0096

As shown in the tight-binding band calculation for [Ni(Et-thiaz**Se**dt)$_2$], the frontier bands exhibit limited dispersions (Figure 6). The calculated band gap was found to be 0.39 eV, which is lower than that of the ethyl dithiolate derivative (0.53 eV).[15] These calculations are in line with the temperature dependence of the resistivity (determined by a two-points procedure given the very small size of the samples). It shows a semiconducting behavior with a room temperature conductivity $\sigma_{RT} = 1.7 \times 10^{-5}$ S.cm^{-1}, and a calculated activation energy of 0.32 eV (Figure S5). This high resistivity associated with the large band gap is essentially a consequence of the strong dimerization, with very limited interactions between dimers.

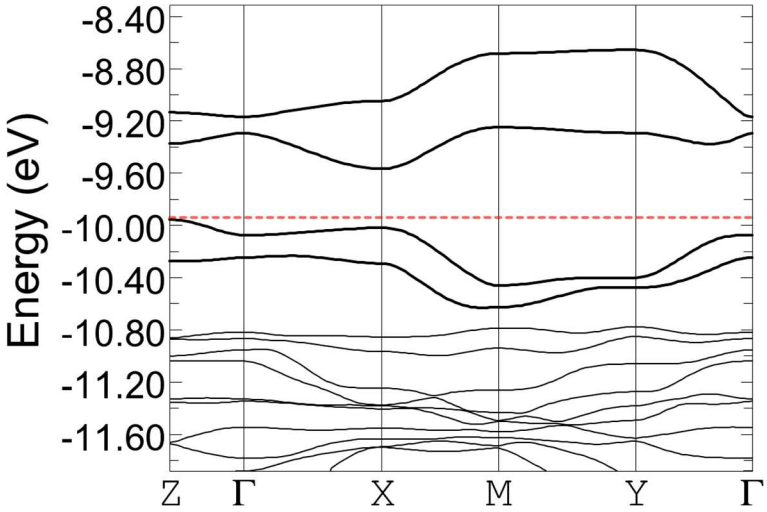

Figure 6 Calculated band structure of [Ni(Et-thiaz**Se**dt)$_2$]$_2$. The dashed line represents the higher occupied level. Γ, X, Y, Z, M, refer to Γ = (0, 0, 0), X = (1/2, 0, 0), Y = (0, 1/2, 0), Z = (0, 0, 1/2), M = (1/2, 1/2, 0), of the Brillouin zone of the triclinic lattice.

The second investigated neutral compound, that is the bis(selenolene) complex [Ni(thiaz**ds**)$_2$] also crystallizes in the triclinic system, space group $P\bar{1}$, but the unit cell contains two crystallographically independent molecules, with both nickel atoms (Ni1, Ni2) on inversion centers. As for [Ni(thiaz**Se**dt)$_2$]$^{-1,0}$ complexes, intramolecular bond distances (Table 3) confirm the oxidized character with the shortening of the C=C bonds and concomitant lengthening of the C–Se bonds, while the effect on the Ni–Se bonds is limited. Complexes are organized into homo-stacks, that is chains of Ni1 complexes running along *a*, alternating in the *b* direction with chains of Ni2 complexes (Figure 7). Electronic interactions between the layers along the third *c*-direction are very weak, as the outer sulfur atom of the thiazoline-2-thione ring is facing an ethyl group in the neighboring layer, giving this compound a strong 2D character. Within each stack, the complexes form uniform chains, with a plane-to-plane distance of 3.66 and 3.60 Å for Ni1 and Ni2 stacks respectively

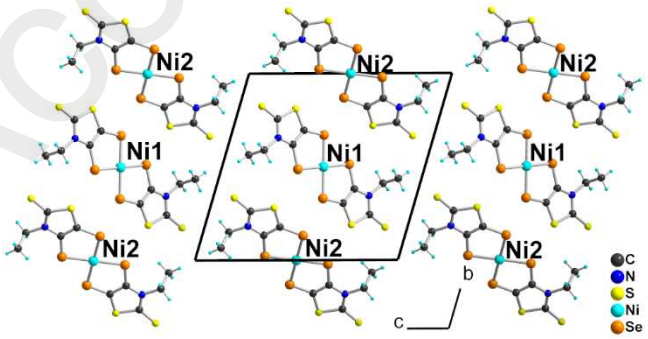

Figure 7 Projection view of the unit cell of [Ni(Et-thiaz**ds**)$_2$] along *a*.

The two independent uniform stacks are associated into layers to give a structural arrangement which can be described as an α-phase, by analogy with BEDT-TTF cation radical salts, with complexes being at a 130° angle from each other (Figure 8). This arrangement generates four different intermolecular interactions, noted I-IV in Figure 8. Calculations of the intermolecular interaction energies (Table 5) indicate that the LUMO provides strongly 1D electronic interactions (interactions I and II), while the HOMO is associated with limited overlaps. Note that the strongest interactions are actually twice as large as those found in the all-sulfur analog [Ni(Et-thiazdt)$_2$], demonstrating the efficiency of the diselenolene approach to favor stronger overlap interactions.

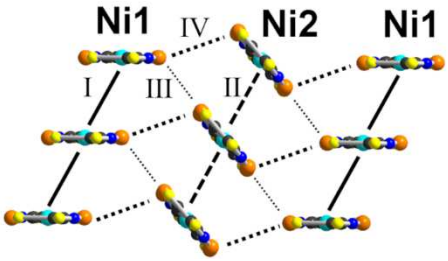

Figure 8. Intra- and interstack interactions of [Ni(Et-thiaz**ds**)$_2$]

Table 5 Values of intermolecular interaction energies of [Ni(Et-thiaz**ds**)$_2$] (in eV)

	HOMO -HOMO	HOMO -LUMO-	LUMO -HOMO	LUMO -LUMO
Int **I**	–0.0250	+0.2787	–0.2297	+0.2787
Int **II**	+0.0385	–0.2960	+0.2960	–0.2530
Int **III**	–0.0446	+0.0280	+0.01350	–0.0258
Int **IV**	+0.0267	–0.0165	–0.0032	–0.0271

As a consequence, the calculated tight-binding band structure (Figure 9) of [Ni(Et-thiaz**ds**)$_2$] shows two narrow HOMO-based bands and two LUMO-based ones with notable dispersions along the stacking direction only, and with a calculated direct band gap at the Γ point of 0.1 eV.

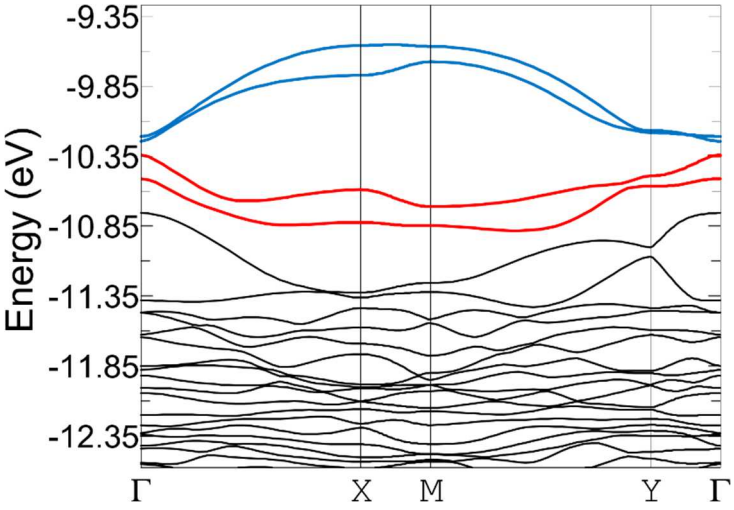

Figure 9. Calculated band structure of [Ni(Et-thiaz**ds**)$_2$], where the HOMO based bands represented in red and the LUMO ones in blue. Γ, X, Y, M, refer to Γ = (0, 0, 0), X = (1/2, 0, 0), Y = (0, 1/2, 0), M = (1/2, 1/2, 0), of the Brillouin zone of the triclinic lattice.

Transport measurements for this compound show that it behaves as a semiconductor at ambient pressure, as expected from the band structure, with $\sigma_{RT} = 8\times10^{-3}$ S.cm^{-1} with E_{act} = 0.12 eV. This conductivity value is on the same order of magnitude as that found in the all-sulfur Ni(Et-thiazdt)$_2$ albeit the structures are different. [Ni(Et-thiazdt)] has been reported to turn metallic below 100 K when the pressure reaches 4.4 GPa, while a further increase of the pressure to 6.9 GPa turns it metallic over the whole temperature range. Furthermore, we also notice on the band structure (Figure 9) the opposite curvature of the HOMO and LUMO bands around the Γ point. This lets us infer that this compound could lead to interesting behaviors (band crossing toward a metallic state, or Dirac cone structure formation) if one is able to increase the bands dispersion up to the point where the two bands would get close enough to each other. In order to evaluate these possibilities, transport measurements under pressure were undertaken here with [Ni(Et-thiaz**ds**)$_2$] using a diamond anvil cell (DAC). Note that the pressure generated by a DAC tends to be anisotropic and its effect is often different from that of hydrostatic pressure. Some of us have developed a DAC technique that can generate high-quality quasi-hydrostatic pressures, as reported earlier[20,21] and used in the present work. As shown in Figure 10a, following a first resistivity drop upon pressure application, a plateau is reached up to 8-9 GPa. Furthermore, when the pressure is increased to 9.5 GPa, an abrupt decrease in resistivity occurs (Figure 10b), while conserving the semiconducting behavior. Further increase of pressure to 11 GPa abruptly decreased the resistivity by another order of magnitude with σ_{RT}(p = 11 GPa) = 36 S.cm^{-1}, and a very small activation energy of 13 meV.

This behavior was not modified at pressures up to 19.1 GPa (See Figure S6). The abrupt change around 10-11 GPa, observed recurrently on several samples on the resistivity also affects in the same way the activation energy (Figure S7) and is therefore suggesting the possibility of an electronic and/or structural transition. Such a transition does not allow us to tentatively follow by calculations the evolution of the band structure under pressure. Below 10 GPa, the relative stability of the conductivity might indicate the possibility of an avoided crossing at the Γ point, as already observed in another nickel bis(dithiolene) complex.[13f]

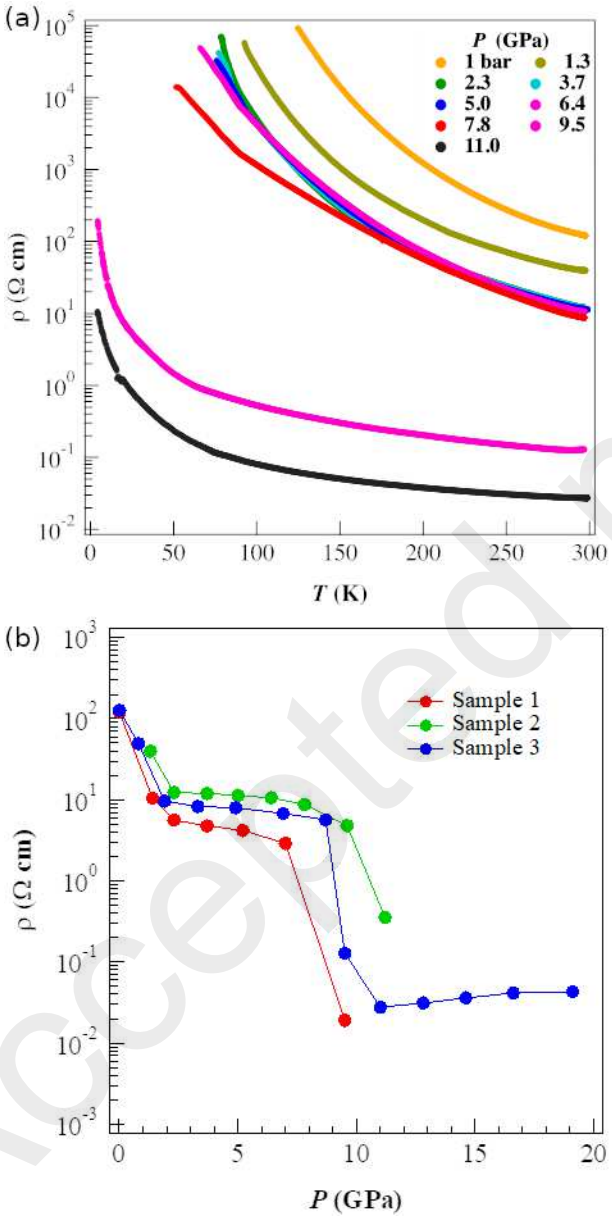

Figure 10 (a) Temperature dependence of the resistivity of [Ni(Et-thiaz**ds**)$_2$] as a function of pressure determined at 1 bar (sample 1), from 2.3 to 7.8 GPa (sample 2) and at 9.5 and 11 GPa (sample 3). Curves at higher pressures (up to 19.1 GPa) are essentially identical to those shown

here at 11 GPa (See Figure S6 for details) (b) Pressure dependence of the room temperature resistivity of [Ni(Et-thiaz**ds**)$_2$] on the three different samples.

■ CONCLUSION

In conclusion, we have prepared two new selenated analogs of the all-sulfur [Ni(Et-thiazdt)$_2$] complex and fully characterized their precursor radical anions. Introduction of a selenone moiety in replacement of the thione to give the neutral [Ni(Et-thiaz**Se**dt)$_2$] complex deeply modifies the solid state organization as an unprecedented (for neutral nickel complexes) strongly dimerized structure is stabilized with a perfectly eclipsed relative orientation in the dimer and very short Se•••Se contacts (81% of the van der Waals contact distance). Limited interactions between dimers leads to a large semiconducting gap and low conductivity (σ_{RT} = 1.7×10^{-5} S.cm^{-1}). On the other hand, going from the neutral [Ni(Et-thiazdt)$_2$] dithiolene to the corresponding [Ni(Et-thiaz**ds**)$_2$] diselenolene complex gives rise to a typical layered structure built out of uniform stacks of the diselenolene complexes, different however from the all-sulfur analog [Ni(Et-thiazdt)$_2$]. Band structure calculations show an essentially 1D electronic structure with large band dispersion and the small band gap. Under high pressures (up to 19 GPa), the conductivity increases by four orders of magnitude and the activation energy is decreased from 120 meV to only 13 meV. The abrupt change observed around 10 GPa suggests a structural phase transition under pressure.

■ EXPERIMENTAL SECTION

General Considerations. Chemicals and materials from commercial sources were used without further purification. All the reactions were performed under an argon atmosphere. Melting points were measured on a Kofler hot-stage apparatus and are uncorrected. Mass spectra were recorded by the Centre Régional de Mesures Physiques de l'Ouest, Rennes. Methanol, acetonitrile and dichloromethane were dried using an Inert pure solvent column device. NMR spectra were recorded at room temperature using $CDCl_3$ unless otherwise noted. Chemical shifts are reported in ppm and ^{1}H NMR spectra were referenced to residual $CHCl_3$ (7.26 ppm) and ^{13}C NMR spectra were referenced to $CHCl_3$ (77.2 ppm). CVs were carried out on a 10^{-3} M solution of complex in CH_2Cl_2 with 0.1 M NBu_4PF_6. Potentials were measured *vs.* SCE as reference electrode. The spectroelectrochemical setup was performed in CH_2Cl_2 with Bu_4NPF_6 0.2 M using a Pt grid as the working electrode, a Pt wire as the counter electrode and SCE reference electrode. A Shimadzu 3600 spectrophotometer was employed to record the UV-vis-

NIR spectra. The N-Et-1,3-thiazoline-2-thione **1**[33] and the proligand **4**,[16] were prepared as previously reported. Elemental analyses were performed at Institut de Chimie des Substances Naturelles (CNRS, Gif/Yvette, France).

Synthesis of 3-ethylthiazole-2(3H)-selenone 2. To a solution of 3-ethyl-1,3-thiazoline-2-thione **1** (2 g, 13.7 mmol) in dry acetonitrile (50 mL), iodomethane (1.7 mL, 27.3 mmol) was slowly added. The reaction was stirred at 50°C for 12 hours under inert atmosphere. The solution was then evaporated affording a crystalline solid. The solid was added to a freshly prepared solution of sodium hydrogenoselenide (NaHSe) [prepared from sodium borohydride (1.2 g, 31.7 mmol) and selenium powder (2.2 g, 27 mmol)] in ethanol under inert atmosphere. After stirring for 1 hour, the solution was added to a 10% acetic acid solution (100 mL). Ethanol was evaporated and the medium was extracted with dichloromethane. The organic phase was washed with water (2 × 200 mL) and dried over $MgSO_4$, The solvent was then evaporated affording **2** as a yellowish oil. Yield: 92%; R_f = 0.60 (SiO_2, CH_2Cl_2). ^{1}H NMR (300 MHz) δ 7.22 (d, *J* = 4.4 Hz, 1H, CH), 6.86 (d, *J* = 4.4 Hz, 1H, CH), 4.29 (q, *J* = 7.3 Hz, 2H, CH_2), 1.40 (t, *J* = 7.3 Hz, 3H, CH_3). ^{13}C NMR (75 MHz) δ 14.1 (CH_3), 47.6 (CH_2), 116.1 (C=C), 132.74 (C=C), 179.3 (C=Se). HRMS (ESI) calcd. for $C_5H_7NNaS^{80}Se^+$: 215.93566, found : 215.9358.

Synthesis of 3-ethylthiazole-4,5-(thio-2-cyanoethyl)-2(3H)-selenone 3. To a −10 °C cooled solution of **2** (1 g, 5.2 mmol) in dry THF (60 mL) was added a freshly prepared LDA solution in THF (7.8 mmol). After stirring for 30 min at −10 °C, sulfur S_8 (0.25 g, 7.8 mmol) was added and the solution was stirred for an additional 30 min. To the medium, a solution of fresh LDA (10.4 mmol) was added, the reaction was then stirred at −10 °C for 3h, followed by addition sulfur S_8 (0.33 g, 10.3 mmol). After 30 min, 3-bromopropionitrile (4.3 mL, 52 mmol) was added dropwise and the reaction mixture was stirred overnight. The solvent was evaporated in *vacuo*, and the residue was washed with water and extracted with CH_2Cl_2. The organic phase was then washed with water and dried over $MgSO_4$. The solvent was evaporated and the concentrated solution was purified by flash chromatography on silica gel using CH_2Cl_2 as eluent to afford **3** as a dark brown powder which is recrystallized from ethanol into yellow crystals. Yield: 37%; mp 128 °C; R_f = 0.25 (SiO_2, CH_2Cl_2). ^{1}H NMR (300 MHz) δ 4.58 (q, *J* = 7.1 Hz, 2H, NCH_2), 3.16 (m, 4H, CH_2), 2.74 (m, 4H, CH_2), 1.40 (t, *J* = 7.1 Hz, 3H, CH_3). ^{13}C NMR (75 MHz) δ 181.2 (C=Se), 136.6 (C=C), 130.1 (C=C), 117.0 (CN), 47.2 (NCH_2), 32.4 (SCH_2), 31.5 (SCH_2), 18.7 ($\underline{CH_2}CN$), 18.6 ($\underline{CH_2}CN$), 13.5 (CH_3). HRMS (ESI) Calcd. for $C_{11}H_{13}N_3\,NaS_3{}^{80}Se^+$:

385.9329, Found: 385.9332. Elem. Anal. Calcd. for $C_{11}H_{13}N_3S_3Se$: C, 36.46; H, 3.62; N, 11.60; S, 26.54. Found: C, 36.25; H, 3.52; N, 11.36; S, 26.98.

Synthesis of [NBu_4][Ni(Et-thiazSedt)]. Under inert atmosphere, a solution of Na (38 mg, 1.65 mmol) in MeOH (20 mL) was added to the protected derivative **3** (200 mg, 5.5 mmol). After complete dissolution, the solution was stirred for 30 mn at room temperature. Then a solution of $NiCl_2 \cdot 6H_2O$ (66 mg, 27.7 mmol) in MeOH (5 mL) was added. Six hours later, a solution of NBu_4Br (200 mg, 0.62 mmol) in MeOH was added affording a precipitate. After stirring for 15 h, the formed precipitate was filtered and recrystallized from DCM/MeOH 20/80 to afford the monoanion complex as dark red crystals. Yield: 31% (70 mg). Mp = 160°C. MS (TOF MS ES) calcd. for $[C_{10}H_{10}N_2NiS_6Se_2]^{-1}$: 567.68 Found: 567.68. Elem. Anal. Calcd. for $C_{26}H_{46}N_3NiS_6Se_2$: C, 38.57; H, 5.73; N, 5.19; S, 23.76; found: C, 38.04; H, 5.39; N, 5.03; S, 23.61.

Synthesis of [PPh_4][Ni(Et-thiazds)$_2$]. Under inert atmosphere, a solution of Na (46 mg, 2 mmol) in MeOH (20 mL) was added to the protected diselenolene derivative **4** (270 mg, 0.66 mmol). After complete dissolution, the solution was stirred for 30 mn at room temperature. Then a solution of $NiCl_2 \cdot 6H_2O$ (80 mg, 0.33 mmol) in MeOH (5 mL) was added, 6 hours later a solution of PPh_4Br (280 mg, 0.67 mmol) in MeOH was added affording a precipitate. After stirring for 15 h, the formed brown yellow precipitate was filtered and recrystallized from DCM/MeOH 20/80 to afford the monoanionic complex [PPh_4][Ni(Et-thiazds)$_2$] as brown yellow crystals. Yield: 52% (172 mg). Mp = 190°C. HRMS (ESI) Calcd for $[C_{10}H_{10}N_2S_4{}^{58}Ni^{80}Se_4]^-$: 663.57466 Found: 663.5737. Elem. Anal. Calcd. for $C_{34}H_{30}N_2NiPS_4Se_4$: C, 40.82; H, 3.02; N, 2.80; S, 12.82; found: C, 40.75; H, 3.02; N, 2.83; S, 13.17.

Electrocrystallizations

[Ni(Et-thiazSedt)]. Under inert conditions in a two-compartment electrocrystallization cell equipped with Pt electrodes, Et_4NPF_6 (200 mg) and [Bu_4N][Ni(Et-thiaz**Se**dt)$_2$] (10 mg) were dissolved in freshly distilled 1,1,2-tricholoroethane (10 mL). The current intensity was adjusted to 0.5 μA, and the reaction was left during seven days. Crystals of the neutral Ni complex were collected on the anode as small plates.

[Ni(Et-thiazds)$_2$]. Under inert conditions in a two-compartment electrocrystallization cell equipped with Pt electrodes, Et_4NPF_6 (200 mg) and [PPh_4][Ni(Et-thiaz**ds**)$_2$] (10 mg) were dissolved in a mixture of CH_3CN/CH_2Cl_2 (7/2, 10 mL). The current intensity was adjusted to 0.5 μA, and the reaction was left during seven days. Crystals of the neutral Ni complex were collected on the anode as small plates. HRMS (ESI) Calcd for $[C_{10}H_{10}N_2S_4{}^{58}Ni^{80}Se_4]^{\cdot-}$: 663.5746; found: 663.5733.

X-Ray Crystallography. Data collections were performed on an APEXII Bruker-AXS diffractometer equipped with a CCD camera for all structures except that of [Bu_4N][Ni(Et-thiazSedt)$_2$] which was recorded on a XtaLAB AFC11 Rigaku diffractometer. Structures were solved by direct methods using the *SIR97* program,[34] and then refined with full-matrix least-square methods based on F^2 (*SHELXL-97*)[35] with the aid of the *WINGX* program.[36] All non-hydrogen atoms were refined with anisotropic atomic displacement parameters. H atoms were finally included in their calculated positions. Details of the final refinements are summarized in Table 6.

Band Structure Calculations.

The tight-binding band structure calculations and $\beta_{HOMO/LUMO}$ interaction energies were based upon the effective one-electron Hamiltonian of the extended Hückel method,[37] as implemented in the Caesar 2.0 chain of programs.[38] The off-diagonal matrix elements of the Hamiltonian were calculated according to the modified Wolfsberg–Helmholz formula [39] All valence electrons were explicitly considered in the calculations and the basis set consisted of double-ζ Slater-type orbitals for the metal and chalcogen atoms, and single-ζ Slater-type orbitals for the rest of the atoms. The exponents, contraction coefficients, and atomic parameters used are collected in Table S1 in ESI.

Table 6 Crystallographic data

	$[Bu_4N]$ $[Ni(Et\text{-}thiazSedt)_2]$	$[Ph_4P]$ $[Ni(Et\text{-}thiazds)_2]$	$[Ni(Et\text{-}thiazSedt)_2]$	$[Ni(Et\text{-}thiazds)_2]$
Formulae	$C_{25}H_{42}N_3NiS_4Se_2$	$C_{34}H_{30}N_2NiPS_4Se_4$	$C_{10}H_{10}N_2NiS_6Se_2$	$C_{10}H_{10}N_2NiS_4Se_4$
FW ($g.mol^{-1}$)	807.61	1000.36	567.19	660.99
System	triclinic	triclinic	triclinic	triclinic
Space group	$P\bar{1}$	$P\bar{1}$	$P\bar{1}$	$P\bar{1}$
a (Å)	8.6970(3)	12.3455(6)	7.6322(8)	4.5320(9)
b (Å)	13.4121(4)	13.0840(6)	9.1574(10)	14.053(3)
c (Å)	16.8380(5)	13.5907(6)	12.9898(14)	14.570(3)
α (deg)	106.481(3)	62.4320(10)	79.505(3)	105.807(6)
β (deg)	95.677(3)	76.185(2)	86.661(3)	92.767(6)
γ (deg)	91.328(3)	77.479(2)	69.440(3)	98.228(6)
V ($Å^3$)	1871.43(11)	1875.28(15)	835.81(16)	879.9(3)
T (K)	293(2)	296(2)	296(2)	296(2)
Z	2	2	2	2
D_{calc} ($g.cm^{-1}$)	1.437	1.772	2.254	2.495
μ (mm^{-1})	2.818	4.692	6.256	9.841
Total refls	25901	28601	10462	6484
Abs corr	multi-scan	multi-scan	multi-scan	multi-scan
T_{min}, T_{max}	0.674,1.252	0.377, 0.450	0.165, 0.687	0.252, 0.906
Uniq refls (R_{int})	8937 (0.0374)	8549 (0.0394)	3793 (0.05)	3978 (0.0562)
Uniq refls ($I > 2\sigma(I)$)	4712	5514	2183	1862
R_1, wR_2	0.0714, 0.1789	0.044, 0.0876	0.0472, 0.0963	0.0676, 0.1443
R_1, wR_2 (all data)	0.1432, 0.2104	0.0901, 0.1038	0.1091, 0.1174	0.163, 0.1919
GOF	1.02	1.029	1.003	0.946
Res. Dens.	0.084, –0.778	1.506, –0.682	0.693, –0.809	1.063, –1.346

Magnetic susceptibility measurements.

The magnetic susceptibility measurements were obtained from Quantum Design SQUID magnetometer, operating between 1.8 and 400 K for dc applied fields ranging from –5 to 5 T. Measurements were performed on polycrystalline samples of [Ni(Et-thiaz**Se**dt)$_2$] (11 mg) at 0.1T, and [Ni(Et-thiaz**ds**)$_2$] (22.5 mg) at 0.5 T. The magnetic data were corrected for the sample holder and the diamagnetic contributions.

Resistivity measurements.

Due to the very small size of the crystals, temperature dependence of the resistivity of [Ni(Et-thiaz**Se**dt)$_2$] was measured by the two-point technique. On the other hand, single crystals of [Ni(Et-thiaz**ds**)$_2$] (average size $0.12 \times 0.04 \times 0.01$ mm^3 for samples 1 and 2, and $0.08 \times 0.02 \times 0.01$ mm^3 for sample 3) were used for the high-pressure resistivity measurements. Current was measured perpendicular to the (bc) plane, along the stacking axis (see Fig. S8 for details). The sample was mounted in the DAC by using the same technique as that used for [Ni(ptdt)$_2$].[40] The sample was encapsulated with a mixture of epoxy and alumina. The diamonds with culet size of 0.7 mm (for sample 1, 2) and 0.56 mm (for sample 3) were used. Electrical contacts were obtained by attaching four gold wires (ϕ10 or 5 μm) with gold paint, and the four-probe DC method was used for all measurements. Daphne Oil 7373 was used as the pressure transmitting medium. The pressure was determined by the shift in the ruby fluorescence *R*1 lines at room temperature.

■ ASSOCIATED CONTENT

Supporting Information

The Supporting Information is available free of charge at XXXXX

Figures S1-S10 and Table S1 (PDF).
Cartesian coordinates for the calculated structures (XYZ)

Accession Codes

CCDC 2058067-2058070 contain X-ray crystallographic files in CIF format for this paper. These data can be obtained free of charge via www.ccdc.cam.ac.uk/data_request/cif, or by emailing data_request@ccdc.cam.ac.uk, or by contacting The Cambridge Crystallographic Data Centre, 12 Union Road, Cambridge CB2 1EZ, UK; fax: + 44 1223 336033

■ AUTHOR INFORMATION

Corresponding authors

Dominique Lorcy – *Univ Rennes, CNRS, ISCR (Institut des Sciences Chimiques de Rennes) - UMR 6226, F-35000 Rennes, France;* orcid.org/ 0000-0002-7698-8452;

Email: dominique.lorcy@univ-rennes1.fr

Marc Fourmigué – *Univ Rennes, CNRS, ISCR (Institut des Sciences Chimiques de Rennes) - UMR 6226, F-35000 Rennes, France ;* orcid.org/0000-0002-3796-4802;

Email: marc.fourmigue@univ-rennes1.fr

Reizo Kato – *Condensed Molecular Materials Laboratory, RIKEN, Wako-shi, Saitama 351-0198, Japan*, orcid.org/0000-0002-2606-4657; Email: reizo@riken.jp

Authors

Hadi Hachem – *Univ Rennes, CNRS, ISCR (Institut des Sciences Chimiques de Rennes) - UMR 6226, F-35000 Rennes, France*

HengBo Cui – *Condensed Molecular Materials Laboratory, RIKEN, Wako-shi, Saitama 351-0198, Japan*

Olivier Jeannin – *Univ Rennes, CNRS, ISCR (Institut des Sciences Chimiques de Rennes) - UMR 6226, F-35000 Rennes, France*

Frédéric Barrière – *Univ Rennes, CNRS, ISCR (Institut des Sciences Chimiques de Rennes) - UMR 6226, F-35000 Rennes, France*

■ ACKNOWLEDGMENTS

This work was supported in part by Université de Rennes 1 (PhD grant to H. H.) and by the JSPS KAKENHI (Grant Number JP16H06346). The stay of H. H. to RIKEN was supported in part by RIKEN International Program Associate and by Rennes Métropole. We thank Takaaki Minamidate (RIKEN) and Thierry Guizouarn (Rennes) for the magnetic susceptibility (SQUID) measurements. This work was granted access to the HPC resources of CINES (France) under the allocation 2020-A0080805032 awarded by GENCI.

■ REFERENCES

[1] Andrews, M. P.; Cordes, A. W.; Douglass, D. C.; Fleming, R. M.; Glarum, S. H.; Haddon, R. C.; Marsh, P.; Oakley, R. T.; Palstra, T. T. M.; Schneemeyer, L. F.; Trucks, G. W.; Tycko, R.; Waszczak, J. V.; Young, K. M.. Zimmerman, N. M. One-dimensional stacking of bifunctional dithia- and diselenadiazolyl radicals: preparation and structural and electronic

properties of 1,3-[(E_2N_2C)C_6H_4(CN_2E_2)] (E = sulfur, selenium). *J. Am. Chem. Soc.*, **1991**, *113*, 3559−3368.

[2] Cordes, A. W.; Haddon, R. C.; Hicks, R. G.; Oakley, R. T.; Palstra, T. T. M.; Schneemeyer L. F.; Waszczak, J. V. Polymorphism of 1,3-phenylene bis(diselenadiazolyl). Solid-state structural and electronic properties of .beta.-1,3-[(Se_2N_2C)C_6H_4(CN_2Se_2)]. *J. Am. Chem. Soc.*, **1992**, *114*, 1729−1732.

[3] Leitch, A. A.; Reed, R. W.; Robertson, C. M.; Britten, J. F.; Yu, X.; Secco R. A.; Oakley, R. T. An Alternating π-Stacked Bisdithiazolyl Radical Conductor *J. Am. Chem. Soc.*, **2007**, *129*, 7903−7914.

[4] (a) Tanaka, H.; Okano, Y.; Kobayashi, H.; Suzuki, W.; Kobayashi, A. A three-dimensional synthetic metallic composed of single-component molecules. *Science* **2001**, *291*, 285–287. (b) Kobayashi, A.; Fujiwara, E.; Kobayashi, H. Single-component molecular metals with extended-TTF dithiolate ligands. *Chem. Rev.* **2004**, *104*, 5243−5264.

[5] (a) Zhou, B.; Idobata, Y.; Kobayashi, A.; Cui, H.; Kato, R.; Takagi, R.; Miyagawa, K.; Kanoda, K.; Kobayashi, H. Single-Component Molecular Conductor [Cu(dmdt)$_2$] with Three-Dimensionally Arranged Magnetic Moments Exhibiting a Coupled Electric and Magnetic Transition. *J. Am. Chem. Soc.*, **2012**, *134*, 12724−12731. (b) Zhou, B.; Ishibashi, S.; Ishii, T.; Sekine, T.; Takehara, R.; Miyagawa, K.; Kanoda, K.; Nishibori, E.; Kobayashi, A. Single-component molecular conductor [Pt(dmdt)$_2$]—a three-dimensional ambient-pressure molecular Dirac electron system. *Chem. Comm.*, **2019**, *55*, 3327−3330. (c) Cui, H.; Kobayashi, H.; Ishibashi, S.; Sasa, M.; Iwase, F.; Kato, R.; Kobayashi, A. A Single-Component Molecular Superconductor. *J. Am. Chem. Soc.*, **2014**, *136*, 7619−7622.

[6] Nunes, J. P. M.; Figueira, M. J.; Belo, D.; Santos, I. C.; Ribeiro, B.; Lopes, E. B.; Henriques, R. T.; Vidal-Gancedo, J.; Veciana, J.; Rovira C.; Almeida, M. Transition Metal Bisdithiolene Complexes Based on Extended Ligands with Fused Tetrathiafulvalene and Thiophene Moieties: New Single-Component Molecular Metals. *Chem. Eur. J.*, **2007**, *13*, 9841−9849.

[7] Pal, S. K.; Itkis, M. E.; Tham, F. S.; Reed, R. W.; Oakley, R. T.; Haddon, R. C. Resonating valence-bond ground state in a phenalenyl-based neutral radical conductor. *Science* **2005**, *309*, 281–284.

[8] Mandal, S.; Samanta, S.; Itkis, M. E.; Jensen, D. W.; Reed, R. W.; Oakley, R. T.; Tham, F. S.; Donnadieu, B.; Haddon, R. C. Resonating valence bond ground state in oxygen-functionalized phenalenyl-based neutral radical molecular conductors. *J. Am. Chem. Soc.* **2006**, *128*, 1982–1994.

[9] (a) Kobayashi, Y.; Terauchi, T.; Sumi, S.; Matsushita, Y. Carrier generation ans electronic properties of a single-component pure organic metal. *Nat. Mater.* **2017**, *16*, 109-114 (b) Kobayashi, Y.; Hirata, K.; Hood, S. N.; Yang, H.; Walsh, A.; Matsushita, Y.; Ishioka, K. Crystal structure and metallization mechanism of the π-radical metal TED. *Chem. Sci*., **2020**, *11*, 11699−11704.

[10] Tian, D.; Winter, S. M.; Mailman, A.; Wong, J. W. L.; Yong, W.; Yamaguchi, H.; Jia, Y.; Tse, J. S.; Desgreniers, S.; Secco, R. A.; Julian, S. R.; Jin, C.; Mito, M.; Ohishi, Y.; Oakley, R. T. The Metallic State in Neutral Radical Conductors: Dimensionality, Pressure and Multiple Orbital Effects. *J. Am. Chem. Soc.,* **2015**, *137*, 14136−14148.

[11] (a) Isono, T.; Kamo, H.; Ueda, A.; Takahashi, K.; Nakao, A.; Kumai, R.; Nakao, H.; Kobayashi, K.; Murakami, Y.; Mori, H. Hydrogen bond-promoted metallic state in a purely organic single-component conductor under pressure. *Nat. Commun*. **2013**, *4*, 1344–1349; (b) Ueda, A.; Yamada, S.; Isono, T.; Kamo, H.; Nakao, A. ; Kumai, R.; Nakao, H.; Murakami, Y.; Yamamoto, K.; Nishio, Y.; Mori, H. Hydrogen-Bond-Dynamics-Based Switching of Conductivity and Magnetism: A Phase Transition Caused by Deuterium and Electron Transfer in a Hydrogen-Bonded Purely Organic Conductor Crystal. *J. Am. Chem. Soc*., **2014**, *136*, 12184−12192.

[12] (a) Schiødt, N. C.; Bjørnholm, T.; Bechgaard, K.; Neumeier, J. J.; Allgeier, C.; Jacobsen, C. S.; Thorup, N. Structural, electrical, magnetic, and optical properties of bis-benzene-1,2-dithiolato-Au(IV) crystals. *Phys. Rev. B* **1996**, *53*, 1773-1778. (b) Schultz, A. J.; Wang, H. H.; Soderholm, L. C.; Sifter, T. L.; Williams, J. M.; Bechgaard, K.; Whangbo, M. H. Crystal structures of bis(5,6-dihydro-1,4-dithiin-2,3-dithiolato)gold and tetrabutylammonium bis(5,6-dihydro-1,4-dithiin-2,3-dithiolato)nickelate(1-) and the ligand like character of the isoelectronic radicals $[Au(DDDT)_2]^0$ and $[Ni(DDDT)_2]^-$. *Inorg. Chem*., **1987**, *26*, 3757−3761; (c) Belo, D.; Alves, H.; Lopes, E. B.; Duarte, M. T.; Gama, V.; Henriques, R. T.; Almeida, M.; Pérez-Benítez, A.; Rovira, C.; Veciana, J. Gold complexes with dithiothiophene digands: A metal based on a neutral molecule. *Chem. Eur. J.* **2001**, *7*, 511−519. (d) Dautel, O. J.; Fourmigué, M.; Canadell, E.; Auban-Senzier, P. Fluorine segregation controls the solid-state organization and electronic properties of Ni and Au dithiolene complexes: stabilization of a conducting single-component gold dithiolene complex. *Adv. Funct. Mater.* **2002**, *12*, 693−698.

[13] (a) Le Gal, Y.; Roisnel, T.; Auban-Senzier, P.; Guizouarn, T.; Lorcy, D. Hydrogen bonding interactions in a single component molecular conductor: hydroxyethyl-substituted radical

gold dithiolene complex, *Inorg Chem* **2014**, *53*, 8755-8761. (b) Filatre-Furcate, A.; Auban-Senzier, P.; Fourmigué, M.; Roisnel, T.; Dorcet, V.; Lorcy, D. Gold dithiolene complexes: easy access to 2-alkylthio-thiazoledithiolate complexes. *Dalton Trans.,* **2015**, *44*, 15683−15689. (e) T. Higashino , T.; Jeannin , O.; Kawamoto , T.; Lorcy , D.; Mori ,T.; Fourmigué , M. A Single-Component Conductor Based on a Radical Gold Dithiolene Complex with Alkyl-Substituted Thiophene-2,3-dithiolate Ligand. *Inorg. Chem.*, 2015, **54** , 9908 —9913 (f) Filatre-Furcate, A.; Bellec, N.; Jeannin, O.; Auban-Senzier, P.; Fourmigué, M.; Íñiguez, J.; Canadell, E.; Brière, B.; Lorcy, D. Single-component conductors: a sturdy electronic structure generated by bulky substituents. *Inorg. Chem.* **2016**, *55*, 6036–6046. (g) Filatre-Furcate, A.; Roisnel, T.; Fourmigué, M.; Jeannin, O.; Bellec, N.; Auban-Senzier, P.; Lorcy, D. Subtle steric differences impact the structural and conducting properties of radical gold bis(dithiolene) complexes. *Chem. Eur. J*. **2017**, *23*, 16004–16013

[14] (a) Branzea, D. G.; Pop, F.; Auban-Senzier, P.; Clérac, R.; Alemany, P.; Canadell, E.; Avarvari, N. Localization versus delocalization in chiral single component conductors of gold bis(dithiolene) complexes. *J. Am. Chem. Soc.* **2016**, *138*, 6838–6851. (b) Andrade, M. M.; Silva, R. A. L.; Santos, I. C.; Lopes, E. B.; Rabaça, S.; Pereira, L. C. J. ; Coutinho, J. T. ; Telo, J. P. ; Rovira, C. ; Almeida, M. ; Belo, D. Gold and Nickel Alkyl Substituted Bis-thiophenedithiolene Complexes: Anionic and Neutral Forms *Inorg Chem Front* **2017**, *4,* 270-280. (c) Mizuno, A.; Benjamin, H.; Shimizu, Y.; Shuku, Y.; Matsushita, M. M.; Robertson, N.; Awaga, K. High Ambipolar Mobility in a Neutral Radical Gold Dithiolene Complex. *Adv. Funct. Mater.,* **2019**, *29*, 1904181.

[15] Tenn, N.; Bellec, N.; Jeannin, O.; Piekara-Sady, L.; Auban-Senzier, P.; Íñiguez, J.; Canadell, E.; Lorcy, D. A single-component molecular metal based on a thiazole dithiolate gold complex. *J. Am. Chem. Soc*. **2009**, *131*, 16961–16967.

[16] Yzambart, G.; Bellec, N.; Nasser, G.; Jeannin, O.; Roisnel, T.; Fourmigué, M.; Auban-Senzier, P.; Íñiguez, J.; Canadell, E.; Lorcy, D. Anisotropic chemical pressure effects in single-component molecular metals based on radical dithiolene and diselenolene gold complexes.*J. Am. Chem. Soc.*, **2012**, *134*, 17138−17148.

[17] Le Gal, Y.; Roisnel, T.; Auban-Senzier, P.; Bellec, N.; Íñiguez, J. Canadell, E.; Lorcy, D. Stable metallic state of a neutral radical single-component conductor at ambient pressure *J. Am. Chem. Soc.*, **2018**, *140*, 6998−7004.

[18] Valade, L.; Legros, J. P.; Bousseau, M.; Cassoux, P.; Garbauskas, M.; Interrante, L.V. Molecular structure and solid-state properties of the two-dimensional conducting mixed-

valence complex $[NBu_4]_{0.29}[Ni(dmit)_2]$ and the neutral $[Ni(dmit)_2]$(H_2dmit = 4,5-dimercapto-1,3-dithiole-2-thione); members of an electron-transfer series. *J. Chem. Soc. Dalton Trans.*, **1985**, 783–794.

[19] Garreau-de Bonneval, B. ; Moineau-Chane Ching, K. I. ; Alary, F.; Bui T.-T.; Valade, L. Neutral d8 metal bis-dithiolene complexes: Synthesis, electronic properties and applications. *Coord. Chem. Rev*., **2010**, *254*, 1457–1467.

[20] Cui, H.; Tsumuraya, T.; Miyazaki, T.; Okano, Y.; Kato, R. Pressure-Induced Metallic Conductivity in the Single-Component Molecular Crystal $[Ni(dmit)_2]$ *Eur. J. Inorg. Chem*., 2014, **24**, 3837–3840.

[21] (a) Filatre-Furcate, A.; Bellec, N.; Jeannin, O.; Auban-Senzier, P.; Fourmigué, M.; Vacher, A.; Lorcy, D. Radical or not radical: compared structures of metal (M = Ni, Au) bis-dithiolene complexes with a thiazole backbone. *Inorg. Chem.*, 2014, **53***,* 8681–8690. (b) Hachem, H.; Cui, H.; Tsumuraya, T.; Kato, R.; Jeannin, O.; Fourmigué, M.; Lorcy, D. Single-component conductors based on closed-shell Ni and Pt bis(dithiolene) complexes: metallization under high pressure. *J. Mater. Chem. C* **2020**, *8*, 11581–11592.

[22] Filatre-Furcate, A.; Barrière, F.; Roisnel, T.; Jeannin, O.; Lorcy, D. Conformational behavior, redox and spectroscopic properties of gold dithiolene complexes: [Au(iPr-thiazYdt)2]-1 (Y = O, S, Se) *Inorg. Chim. Acta* **2018**, *469*, 255-263.

[23] Deiana, C.; Aragoni, M. C.; Isaia, F.; Lippolis, V.; Pintus, A.; Slawin, A. M.; Arca, M. Structural tailoring of the NIR-absorption of bis(1,2-dichalcogenolene) Ni/Pt electrochromophores deriving from 1,3-dimethyl-2-chalcogenoxo-imidazoline-4,5-dichalcogenolates. *New J. Chem*. **2016** *40*, 8206-8210.

[24] Aragoni, M. C.; Arca, M.; Caironi, M.; Denotti, C.; Devillanova, F.A.; Grigiotti, E.; Isaia, F.; Laschi, F.; Lippolis, V.; Natali, D.; Pala, L. Monoreduced $[M(R,R\text{ ' timdt})_2]^-$ dithiolenes (M = Ni, Pd, Pt; R,R ' timdt = disubstituted imidazolidine-2,4,5-trithione): solid state photoconducting properties in the third optical fiber window. *Chem. Commun*., **2004**, 1882–1883.

[25] Mueller-Westerhoff, U. T.; Yoon, D. I.; Plourde, K. Near-IR dyes for the 1.3 to 1.5 micron region – The use of substituted dithiolene complexes. *Mol. Cryst. Liq. Cryst.* **1990**. *183*, 291-302.

[26] Ciancone, M.; Mebrouk, K.; Bellec, N.; Le Goff-Gaillard, C.; Arlot-Bonnemains, Y.; Benvegnu, T.; Fourmigué, M.; Camerel, F.; Cammas-Marion S. Biocompatible

nanoparticles containing hydrophobic nickel-bis(dithiolene) complexes for NIR-mediated doxorubicin release and photothermal therapy. *J. Mater. Chem. B*, **2018** *6*, 1744-1753.

[27] Olk, R.M.; Röhr, A.; Sieler, J.; Köhler, K.; Kirmse, R.; Dietzsch, W.; Hoyer, E.; Olk. B. Coordination chemistry of 1,3-dithiole-2-thione-4,5-diselenolate (dsit) – Comparison with 1,3-dithiole-2-thione-4,5-dithiolate (dmit). *Z. Anorg. Allg. Chem.*, **1989**, *577*, 206-216

[28] (a) Sato, A.; Kobayashi, H.; Naito, T.; Sakai, F.; Kobayashi, A. Enhancement of the Dimensionality of Molecular π Conductors by the Selone Substitution of $M(dmit)_2$ (M = Ni, Pd) Systems: Newly Synthesized dmise Compounds $[Me_xH_{4-x}N][Ni(dmise)_2]_2$ (x = 1−3) and $Cs[Pd(dmise)_2]_2$ (dmise = 4,5-Dimercapto-1,3-dithiole-2-selone). *Inorg. Chem*. **1997**, 36, 5262. (b) Cornelissen, J.P. Pomarede, B. Spek, A.L. Reefman, D. Haasnoot, J.G. Reedijk, J. Two phases of $[Me_4N][Ni(dmise)_2]_2$: syntheses, crystal structures, electrical conductivities, and intermolecular orbital overlap calculations of α- and β-tetramethylammonium bis[bis(2-selenoxo-1,3-dithiole-4,5-dithiolato)nickelate], the first conductors based on the $M(C_3S_4Se)_2$ system. *Inorg. Chem.* **1993**, *32*, 3720-3726. (c) Zuo, J.-L.; Yao, T.-M.; You, X.-Z.; Fun, H.-K.; Kandasamy, S. Syntheses, properties and crystal structures of a series of mixtures of dmit and dmise metal complexes (dmit 1,3-dithiole-2-thione-4,5-dithiolate, dmise 1,3- dithiole -2-selone-4,5- dithiolate). Single-crystal esr study of $[Bu_4N]_2[Cu/Ni(C_3S_{4.4}Se_{0.6})_2]$. *Polyhedron*, **1996**, *15*, 3547-3557.

[29] Matsubayashi, G.; Yokozawa, A. Spectroscopy and electrical conductivity of $[Au(C_3S_5)_2]^{n-}$ and $[Au(C_3Se_5)_2]^{n-}$ (n = 0-1) complexes and X-ray crystal-structure of $[n Bu_4N][Au(C_3S_5)_2]$. *J. Chem. Soc., Dalton Trans*. **1990**, 3013−3019.

[30] The interaction energy between orbitals i and j ($\beta_{i,j}$) can be written as $\beta_{i,j} = \sum_\nu \sum_\mu c_{\nu i} c_{\mu j} \langle \chi_\nu | H^{eff} | \chi_\mu \rangle$, where $c_{\nu i}$ denotes the coefficient of atomic orbital χ_ν in the molecular orbital ψ_i, with $\psi_i = \sum_\nu c_{\nu i} \chi_\nu$.

[31] Williams, J. M.; Wang, H. H.; Emge, T. J.; Geiser, U.; Beno, M. A.; Leung, P. C. W.; Carlson, K. D.; Thorn, R. J.; Schultz, A. J.; Whangbo, M.-H. Rational design of synthetic metal superconductors. *Prog. Inorg. Chem*. **1987**, *35* 51−218.

[32] Canadell, E.; Rachidi, I. E. I.; Ravy, S.; Pouget, J.-P.; Brossard, L.; Legros, J. P. On the band electronic structure of $X[M(dmit)_2]_2$ (X = TTF, $(CH_3)_4N$; M = Ni, Pd) molecular conductors and superconductors. *J. Phys.* **1989**, *50*, 2967−2981.

[33] Roussel, C.; Gallo, R.; Chanon, M.; Metzger, J. Reactions leading to 3,4-dialkyl-Δ_4-2-thiazolinethiones – Influence of steric factors on course of reaction. *Bull. Soc. Chim. Fr.* **1971**, *5*, 1902−1907.

[34] Altomare, A.; Burla, M. C.; Camalli, M.; Cascarano, G.; Giacovazzo, C.; Guagliardi, A.; Moliterni, A. G. G.; Polidori, G.; Spagna, R. SIR97: a new tool for crystal structure determination and refinement. *J. Appl. Cryst*., **1999**, *32*, 115–119.

[35] Sheldrick, G. M. A short history of SHELX. *Acta Crystallogr.,* **2008**, *A64*, 112–122.

[36] Farrugia, L. J. WinGX and ORTEP for Windows: an update. *J. Appl. Cryst*., **2012**, *45*, 849–854.

[37] Whangbo, M.-H., Hoffmann, R. The band structure of the tetracyanoplatinate chain. *J. Am. Chem. Soc.,* **1978**, *100*, 6093−6098.

[38] Ren, J.; Liang, W.; Whangbo, M.-H. Crystal and Electronic Structure Analysis Using CAESAR; PrimeColor Software, Inc.: Cary, NC, 1998.

[39] Ammeter, J.; Burgi, H.-B.; Thibeault, J.; Hoffmann, R. Counterintuitive orbital mixing in semiempirical and ab initio molecular orbital calculations. *J. Am. Chem. Soc.*, **1978**, *100*, 3686−3692.

[40] Cui, H.; Brooks, J. S.; Kobayashi, A.; Kobayashi, H. Metallization of the Single Component Molecular Semiconductor [Ni(ptdt)$_2$] under Very High Pressure. *J. Am. Chem. Soc*., **2009**, *131*, 6358–6359.

For Table of Contents Only

SYNOPSIS. Two selenated analogs of the all-sulfur neutral dithiolene complex [Ni(Et-thiazdt)$_2$] exhibit strikingly different structural and electronic behaviors, (a) eclipsed dimers and short Se•••Se intermolecular contacts in the poorly conducting [Ni(Et-thiaz**Se**dt)$_2$] bearing outer selenone moieties, (b) uniform stacks and high conductivity in the diselenolene [Ni(Et-thiaz**ds**)$_2$] complex. The latter undergoes a conductivity increase by four orders of magnitude (up to 20-30 S cm^{-1}) under high pressure (up to 19 GPa).